Comparing Local and Marching Analyses of Görtler Instability

H. P. Day*
Mount Hood Community College, Portland, Oregon 97218
T. Herbert†
The Ohio State University, Columbus, Ohio 43210
and
W. S. Saric‡
Arizona State University, Tempe, Arizona 85287

Two methods of solving the partial differential equations describing Görtler instability are compared. Local separation-of-variable analysis predicts growth rates independently of any assumptions about initial disturbances. Global marching analysis requires initial-disturbance assumptions but is shown to provide results that are not affected after sufficient marching. The local analysis results are compared to the marching results and are seen to consistently overestimate growth rates by modest amounts. The distance required for different disturbances to collapse onto one common curve is estimated from several examples. The first neutral point cannot be clearly identified by the marching analysis because convergence to the asymptotic curve is too slow and because the most unstable disturbance changes rapidly with streamwise position upstream of the neutral point. Different measures of growth give slightly different results because of the changing disturbance shape.

Nomenclature

f = Blasius boundary-layer function, $U=f'$
G = Görtler number, $=(x/\epsilon R)^{1/2}$
N = growth measure, $=\ell n(u_{m1}/u_{m0})$
p = perturbation pressure
R = radius of curvature of the wall
U_∞ = flow velocity outside the boundary layer
U,V = boundary-layer velocity components, streamwise and normal to wall
u,v,w = perturbation velocity components, streamwise, normal, and spanwise
u_m,v_m = maxima of velocity profiles
$\bar{x}_0$ = streamwise reference length (dimensional)
α = spanwise wavenumber of perturbation, $=\epsilon\cdot 2\pi/\lambda$
α_g,G_g = global value based on $\bar{x}_0$ rather than on $\bar{x}$
β = exponential growth rate, based on peak amplitude of u
γ = exponential growth rate, based on integral of u^2
ϵ = small parameter, $=(\nu/U_\infty\bar{x}_0)^{1/2}$
η = boundary-layer variable, $=y/x^{1/2}$
Λ = nondimensional spanwise wavelength, $=G(2\pi/\alpha)^{3/2}$
λ = dimensional spanwise wavelength
ν = kinematic viscosity
ξ = streamwise variable, $=x^{1/2}$
σ = exponential growth rate, based on integral of $u^2+v^2+w^2$
$\bar{}$ = dimensional values

Introduction

GÖRTLER instability can be responsible for boundary-layer transition and alternately can provide the three-dimensional disturbance that causes breakdown of Tollmien-Schlichting waves. For a large disturbance wavenumber, there is general agreement on the linear theory, and an analytic, asymptotic solution is available.[1] However, for order one wavenumbers when the spanwise disturbance wavelength is on the order of the boundary-layer thickness, most analyses are local, separation-of-variables analyses, and they disagree widely.[2]

Hall[3] argues that all separation-of-variables solutions are wrong and cannot model the two-dimensional stability equations in x and y. Strictly speaking, he is correct. But are such local solutions still useful? There are two questions here: Do different, random disturbances converge to one predictable disturbance (a function of wavelength and position) as they evolve downstream within the region of order one wave-number? If not, no theory giving disturbance growth rates as a function of Görtler number G and wavenumber α is valid here. The second question is if so, how wrong is the local analysis growth rate?

To answer the second question, one wants to solve the stability equations by marching and to compare the disturbance shape and growth rate to local theory. Since marching results vary depending on initial conditions but less so the farther one marches, the problem is to find an *asymptotic disturbance* (a function of wavenumber and Görtler number) to which all disturbances collapse, given sufficient distance. *Asymptotic* is used here in the sense of disturbances converging to each other and not in the sense of wavenumber getting small. In this study, local solutions are used as initial conditions to a marching scheme. Runs are started at different streamwise positions and the disturbances are followed until they collapse onto each other.

The answer to the first question cannot be given without knowing what the variation in initial disturbances is in practice. That requires not only solving the receptivity problem, but knowing the properties of some freestream turbulence or other disturbance as well. The beginning of an answer is reported here by systematically altering initial conditions and by

Received Aug. 15, 1988; revision received Aug. 21, 1989.

*Instructor, Department of Theoretical Mechanics.
†Professor, Departments of Mechanical Engineering and Aeronautical and Astronautical Engineering. Member AIAA.
‡Professor, Department of Mechanical and Aerospace Engineering. Member AIAA.

seeing how soon differences disappear and how much difference an N factor has accumulated.

Problem Statement

In order to focus on the differences between local and marching analyses, a simple Görtler problem is posed. The physical problem is illustrated in Fig. 1. The Blasius boundary layer is used, small curvature is assumed, and the perturbations are assumed linear, steady, and spanwise periodic with a specified wavelength λ.

In the following, x_0 is an arbitrary reference length, chosen in this work as that $\bar{x}$ where local analysis gives onset of instability (the first neutral point).

$$\epsilon = (\nu/U_\infty x_0)^{1/2}$$

$$\bar{x} = x_0 x \qquad \bar{y} = x_0 y, \qquad \bar{z} = \epsilon x_0 z$$

$$\bar{U} = U_\infty U(x,y), \qquad \bar{V} = \epsilon U_\infty V(x,y)$$

$$\alpha_g = \epsilon x_0 2\pi/\lambda$$

$$\bar{u}(x,y,z) = U_\infty u(x,y)\cos\alpha_g z$$

$$\bar{v}(x,y,z) = \epsilon U_\infty v(x,y)\cos\alpha_g z$$

$$\bar{w}(x,y,z) = \epsilon U_\infty w(x,y)\sin\alpha_g z$$

$$\bar{p}(x,y,z) = \rho U_\infty^2 p(x,y)\cos\alpha_g z$$

Note in particular that downstream disturbances to the velocity are scaled differently than components spanwise and normal to the wall. This is reasonable because a weak movement of fluid normal to the wall produces relatively strong boundary-layer shear.

After substitution of the velocity ($\bar{U}+\bar{u}$, $\bar{V}+\bar{v}$, $\bar{w}$) into the Navier-Stokes equations for curved coordinates,[4] subtraction of the base flow, and linearization, terms of higher than first order in curvature and Reynolds number are discarded. (For details see Floryan and Saric.[5]) The resulting x-y stability equations are

$$u_x + v_y + \alpha w = 0$$

$$Uu_x + Vu_y + U_x u + U_y v = u_{yy} - \alpha^2 u$$

$$Uv_x + Vu_y + V_x u + V_y u + 2G^2 Uu = -p_y + v_{yy} - \alpha^2 v$$

$$Uw_x + Vw_y = \alpha p + w_{yy} - \alpha^2 w$$

$$G_g = (x_0/\epsilon R)^{1/2}$$

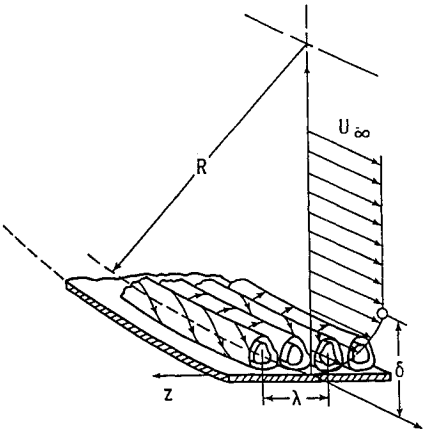

Fig. 1 Problem definition.

Both the Görtler number and wavenumber appear using x_0 as the characteristic length scale. These global values are written G_g and α_g to distinguish them from the local values G and α based on x. Care must be taken in comparing local and marching analyses, as the reference length used in local analyses is $\bar{x}$, the variable of the marching analysis, rather than $\bar{x}_0$. This difference reappears in defining growth rates below. This set of equations forms a consistent first-order approximation to the effect of curvature.

The equations were solved locally by separation of variables by Floryan and Saric,[5] by Ragab and Nayfeh,[6] and globally by numerical marching by Hall.[3] The present numerical scheme follows that of Hall.[3]

Marching Solution

Hall[3] reduced the original four differential equations to two by reducing the dependent variables from (u,v,w,p) to (u,v). This is necessary because no x derivative of p appears in the equations. The full four-equation set cannot be marched. In the strict mathematical sense, it appears that neither the two- nor four-equation set are parabolic. Further, w is not independent of u,v at a streamwise station: one can calculate $w(\eta)$ from $u(\eta)$, $v(\eta)$.

For the sake of an efficient solution, the nondimensional (x,y) coordinates were converted to the coordinates (ξ,η) defined below. The base flow $(U,V,0)$ was expressed in terms of the Blasius function $f(\eta)$:

$$\xi = x^{1/2}, \qquad \eta = y/\sqrt{x}$$

$$f''' + f''f/2 = 0, \qquad f(0) = 0 \qquad f(\infty) \to 1$$

$$U = f', \qquad V = (\eta f' - f)/(2\xi)$$

The final two-equation set, equivalent to Hall's except for the replacement of x with ξ, is

$$2u_{\eta\eta} + fu_\eta - \xi f' u_\xi + (\eta f'' - 2\alpha^2\xi^2)u - 2\xi f'' v = 0$$

$$(\eta^2 f'' - \eta f' + f)u_{\eta\eta} - 2\eta\xi f'' u_{\eta\xi} + (2\eta^2 f''' + 4\eta f'')u_\eta$$
$$- (2\eta\xi f''' + 2\xi g'')u_\xi$$
$$+ [\eta^2 f'''' + 5\eta f''' + 3f'' - \alpha^2\xi^2(\eta^2 f'' + \eta f' - f)$$
$$+ 8\alpha^2\xi^5 G^2 f']u$$
$$+ 4\xi v_{\eta\eta\eta\eta} + 2\xi f v_{\eta\eta\eta} - 2\xi^2 f' v_{\eta\eta\xi} - (2\eta\xi f'' - 4\xi f' + 8\alpha^2\xi^3)v_{\eta\eta}$$
$$- (4\eta\xi f''' + 2\xi f'' + 2\alpha^2\xi^3 f)v_\eta + (2\xi^2 f''' + 2\alpha^2\xi^4 f')v_\xi$$
$$- (2\eta\xi f'''' + 4\xi f''' - 2\alpha^2\xi^3\eta f'' - 4\alpha^4\xi^5)v = 0$$

The marching scheme follows Hall; therefore no detailed description will be given. At each step in the solution, values of u,v at one ξ station are used to find values at the next by matrix inversion. The outer boundary condition was the simple one of setting all perturbation velocities equal to zero at two final grid points, and accuracy was assured by extending the grid far enough from the wall that further changes did not affect the results. For runs starting upwind of the neutral-stability curve, or simply near it for smaller α, this was costly.

Hall's published growth curves and disturbance profiles were accurately reproduced by the programs used in this work.

Growth Measure

Because the disturbances considered change shape as well as strength, different measures of growth give different results. That choice of measure affects, for example, where the neutral-stability curve is located and which of two disturbances is less stable.

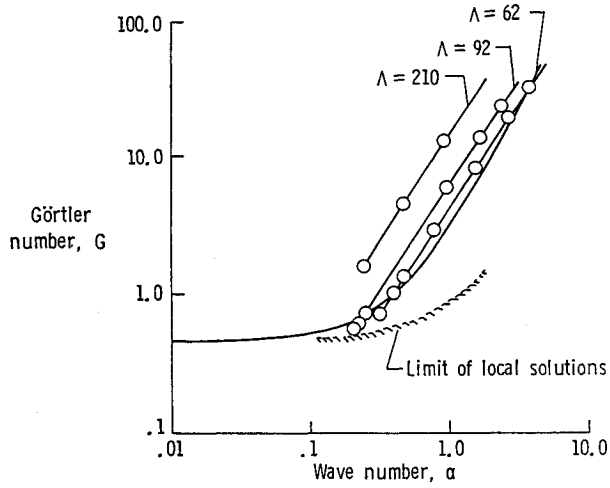

Fig. 2 Wavenumber—Görtler number plane showing paths of constant Λ and starting points for marching with the neutral curve from Floryan and Saric.

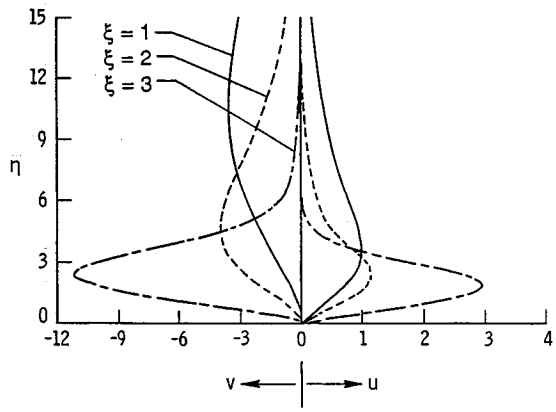

Fig. 3 Successive disturbance velocity profiles showing u,v for $\Lambda = 62$ at $\xi = 1$ (taken from local theory as initial condition) and after marching to $\xi = 2,4$; the computational grid extends to $\eta = 50$.

The growth measures used here are exponential, that is, if $a(x) = a_0 \exp(gx)$ locally, then $g = a'/a$ is the growth rate of $a(x)$. Three choices of $a(x)$ give three different measures:

$$\beta = a'/a, \text{ where } a(x) = \max_y (u)$$

$$\sigma = a'/a, \text{ where } a(x) = \int (u^2 + v^2 + w^2)\, dy$$

$$\gamma = a'/a, \text{ where } a(x) = \int u^2 dy$$

The β also differs from the other two growth rates in using a streamwise coordinate nondimensionalized by the local value of x rather than by the global value x_0. This aids comparison of β with the local analysis results and γ and σ with Hall's results.

The β is the simplest measure of growth but does not account for the thickness of the region of disturbed flow, which changes as the peak in the u profile moves toward or away from the wall.

The σ is Hall's measure of growth and includes the growth of all three components of velocity. This would seem a virtue until one recalls the scaling of these nondimensional velocities. A unit increase in v is smaller in physical terms than a unit increase in u by the order of the thickness Reynolds number at $\tilde{x} = \tilde{x}_0$. Thus not only does this measure give disproportionate importance to v and w, but the relative importance of, say, u and v depends on the arbitrary choice of $\tilde{x}_0$.

The γ approximates the growth of the energy contained in the disturbance. The terms like uU in the expression for energy average out to zero when integrated across one disturbance wavelength. The terms $u^2 + w^2$ are divided by the square of the thickness Reynolds number, as just explained. If they are neglected, we are left with $\int u^2/dy$, whose integral growth is γ.

Marching Results

In this section, runs which start at different ξ but follow the same constant λ curve in the G, α plane are discussed. Several curves of constant λ are shown in Fig. 2, which also shows Floryan and Saric's neutral curve. The nondimensional Λ is defined by

$$\Lambda = G(2\pi/\alpha)^{3/2} U_0/(\nu R^{1/2})$$

The starting point of each of the runs is marked as a circle in Fig. 2.

For each Λ, the runs are overlapped until their disturbances converge to a common one. The properties of that common disturbance are then compared to the predictions of local theory. Initial conditions are provided by Floryan and Saric's separation-of-variable program. For each Λ, the arbitrary x_0 is chosen to fall on the local analysis neutral curve; therefore $\xi = 1$ there.

Figure 3 shows u and v profiles at successive streamwise stations for a typical run starting at $\alpha = 0.4$, $G = 0.998$, $\Lambda = 62$, and $\xi = 1$. The first set of profiles is the starting separation-of-variables solution. Later profiles move toward the wall growing at first and then decaying in amplitude. Corresponding local solutions behave similarly.

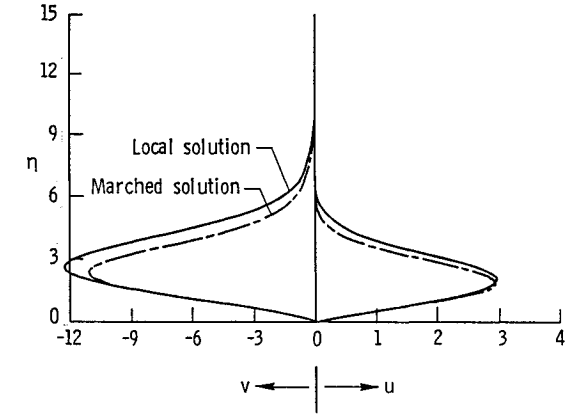

Fig. 4 Comparison beween final profile of Fig. 3 and corresponding local solution.

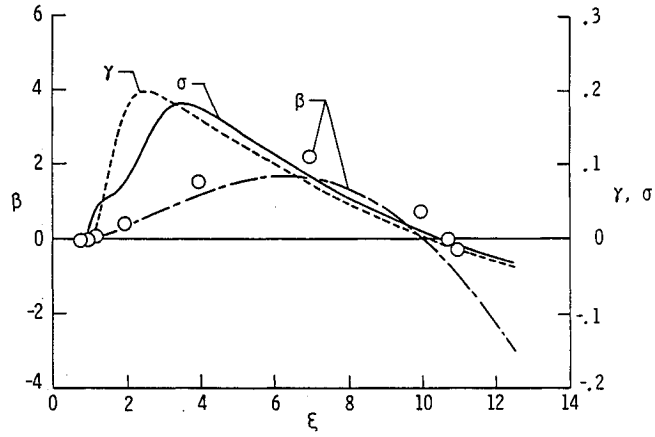

Fig. 5 Growth rates β, γ, and σ for the run of Figs. 3 and 4; the circles show the values of β obtained from local analysis.

The local and the marched solutions for $\xi = 4$ are compared in Fig. 4. The local solution has been normalized; therefore the u amplitudes (u_m) are the same. As ξ increases, local and marched profiles both shift to lower η, though not the same amount. The amplitude ratio v_m/u_m also changes in both, also in somewhat different amounts. A better look at these trends and the differences between local and marched solutions will be given in Figs. 7 and 8.

Figure 5 compares three different measures of growth rate for the run of Fig. 3. It also shows the growth rates predicted by the local analysis, which should be compared with the β curve. The zero crossings of the three curves are typically different, at both the first and second neutral points. In the present case, the three growth measures agree at the first neutral point but only because the disturbance there is initially unchanging. The σ is very sensitive to inaccuracies in representing a mode: an incorrect shape or an η truncation too close to the wall will cause erratic initial behavior. The other two growth measures, depending only on u, are much less sensitive. The difference in shape between β and γ or σ is characteristic and due to the different nondimensionalizations of the x derivatives in the definitions of each.

Figure 6 shows the amplitude u_m as a function of the downstream position for two runs at $\Lambda = 62$. The starting location, of course, affects the disturbance amplitudes and initially the growth rate corresponding to the slope of this curve. Yet after initial changes, the ratio of amplitudes between the two runs does not change. This is seen more clearly in the plots of the growth rate in Fig. 7.

The five graphs in each part of Figs. 7 and 8 show, as a function of ξ, the growth rates β and γ, the logarithm of the peak-amplitude ratio v_m/u_m, the η location of the u and v peaks, and their y location. The σ is similar to λ and is omitted. The μ peak gives a good idea of how far outside the boundary layer a disturbance extends, while the peak y expresses how flat or round the vortex is. The y height of a round vortex, for each of the three cases, would be 8, 13, and 26. In each family of curves, the local modes used as initial conditions are plotted as circles or, in the case of η and y/λ, as a plus for the u profile and an $\times$ for the v profile.

Important points to note in these plots are the initial agreement between the local analysis β and the growth rate found in marching, the initially stationary values of the profile shape, the lag of the marched values behind the local mode values, and the eventual convergence of all runs to one *asymptotic disturbance* for any given Λ and G. The facts that initially the disturbance behavior is constant-shape and that local analysis accurately predicts the initial growth found in marching give confidence in both treatments of the basic equations.

The lag of the marched v_m/u_m and y_m behind the local solution values indicates that the local solution provides a *moving target* in terms of these values, which the marching solution is always moving toward but never reaches. This makes sense

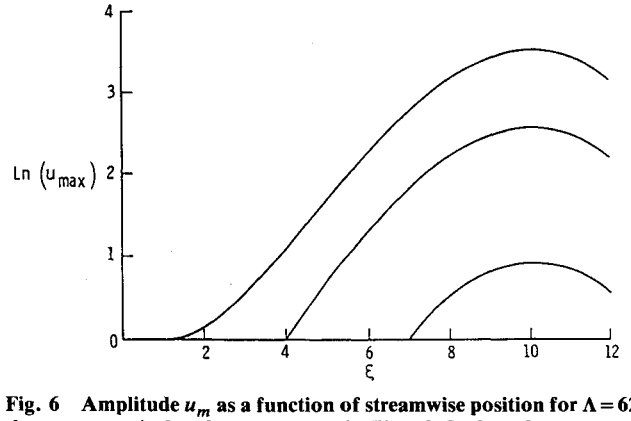

Fig. 6 Amplitude u_m as a function of streamwise position for $\Lambda = 62$; the top curve is for the run shown in Figs. 3–5; the other two runs were started farther downstream.

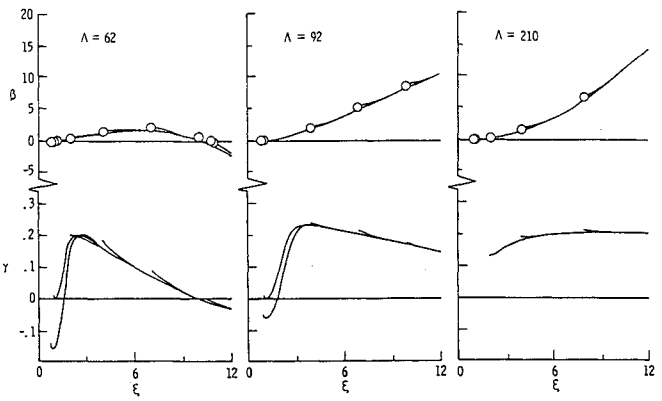

Fig. 7 Three Λ families of runs for $\Lambda = 62, 92, 210$; plotted as a function of ξ are β (top) and γ (bottom).

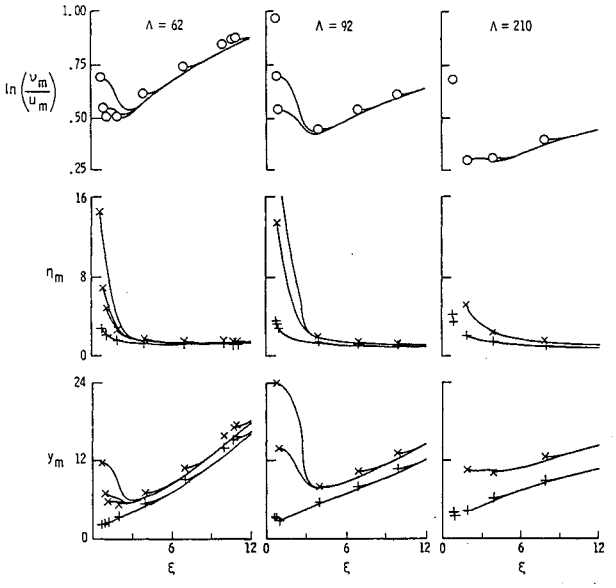

Fig. 8 Three Λ families of runs for $\Lambda = 62, 92, 210$; plotted as a function of ξ are v_m/u_m (top), η_m (middle), and γ_m (bottom). In the latter two graphs, maximum positions of u and v are denoted by + and $\times$, respectively.

physically and explains the fact that the marched growth rates fall below the local growth rates: the marched disturbances never quite reach the target. What one sees here is that local analysis asks what is the most unstable, shape-preserving disturbance at some location, whereas marching analysis asks what shape results at this location from the *filter* of the upstream history.

The local solutions show v_m moving away from the wall as one moves upstream of the local-analysis neutral curve. This is not only true in terms of η as one would expect, but also in terms of y, and the vortices become tall, thin shear layers before the code fails to find solutions (below the dashed line in Fig. 2). This trend runs against intuition and suggests a breakdown of the local theory. It also prevents the marching code from starting at $\xi = 1$ for the case of $\Lambda = 210$. Though the local analysis can use an asymptotic behavior of disturbances outside the boundary layer and need not integrate farther than the boundary-layer edge, the marching analysis needs to extend its η grid out until v is about 5% of its maximum value in order not to change the results more than a few percent. Thus the present marching code, lacking any asymptotic behavior for large η, is unable to use local solutions over a large region of Fig. 2. This is, however, a region where the local solutions are suspect.

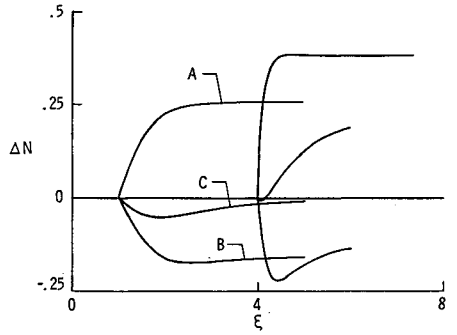

Fig. 9 Effect of changing disturbance shape on subsequent growth factor N; three pairs of runs with different initial conditions are started at two different streamwise positions.

Varying Initial Conditions

How do variations in the initial disturbances affect growth rates? How far downstream do different disturbances converge to the same solution? How much have the differences affected the disturbance amplitude by the time they have no further effect on growth?

In this section, pairs of initial conditions are marched to see what effect their difference has on the final disturbance amplitude and how long one must march to get identical growth rates. The first disturbance of a pair is the local solution, and the second is derived from the first by altering the ratio v_m/u_m and the η scaling of the u and v profiles.

The values of u_m for the second run of each pair were divided by corresponding values from the first run and the ratio plotted agains ξ. One would expect this ratio to reach a limiting value, and it is of interest to know both what this value is and how long it takes to reach this limit. The sample curves in Fig. 9 show the effect of varying v_m/u_m, then η_m of the v profile, then both together. Comparisons are made starting at two separate streamwise stations, at $\Lambda = 62$. Other runs were made varying the amount the profile was distorted, the type of distortion, and the values of ξ and Λ. Several observations can be made.

Some altered profiles actually grow more than the local *optimum*. Thus these local solutions are not upper bounds on possible growth in apparent contradiction to the earlier statement regarding marched growth rates falling below local solutions. The altered disturbances which do grow faster rapidly change their shapes and lose their advantage converging to the asymptotic curve established by marching. But they leave a net gain, and because of their shape change, they cannot be discovered by separation of variables.

The amount of initial distortion affects the net gain or loss of amplitude. And for the case where v_m/u_m is altered, one would like to know how wrong an N factor analysis of Görtler vortex growth can be, if some kinds of disturbances can cause more growth than either local theory or marching from a local solution would show, and if so, how much more. For $\Lambda = 62$, starting at $\xi = 1$, a quadrupling of the local solution's v_m/u_m causes a net gain of 0.6 in N factor.

In practice, disturbances with larger v_m/u_m are likely to have smaller u_m; therefore though an N factor expressing u_m growth may be unusually large for these disturbances, the actual final amplitude will not be. If one compared several runs with the same initial v_m instead of the same u_m, large v_m/u_m would not be an advantage. Since u and v perturbations are of comparable magnitude in freestream turbulence, in contrast to the small value of v_m/u_m for Görtler vortices, one would expect the receptivity problem to be governed by the v values introduced into the boundary layer, rather than the u.

Starting farther downstream usually magnifies the effect of an alteration, but overall growth is more when starting near the local theory neutral point in the cases studied. The ξ interval needed to converge tends to decrease with increasing ξ as seen in Fig. 9, but the x interval sometimes increases. The distance required for collapse does not depend on amplitude of alteration but varies with what aspect is altered and is increased if several kinds of changes are combined.

Better conclusions must wait for clarification of what disturbances will be imposed on the boundary layer by external sources.

Locating the First Neutral Point

A specific issue raised by the convergence question is whether the first neutral point can be defined by marching. The need is to start far enough upstream of the neutral point to demonstrate convincingly that a variety of initial conditions do in fact converge to the same disturbance before that disturbance becomes unstable.

Figure 8 shows several runs started at or before the local solution's neutral point. Note that v_m and v_m/u_m for the local solutions both change so rapidly with x that the farther upstream we start, the farther downstream a disturbance converges to the asymptotic limit. Also, there is a lower G limit (hence ξ limit) for each Λ before which Floryan's program is unable to find a mode (see Fig. 2). The earliest starting points in Fig. 8 are close to that limit. Thus the present work fails to establish by marching where the first neutral point should fall. The culprit is not heightened sensitivity or reduced convergence rate. It is the rapid variation of the local solution with x.

The difficulty in locating the first neutral point reflects the wide disparity in analytical results concerning the neutral curve.[2] The breakdown of the local analysis for small ξ raises the question whether the rapid variation of profile shape can be attributed to the partial differential equation themselves or to the local solution method. If the former, then it will not be possible to define a first neutral curve for these equations nor would such a curve, if it were definable, be meaningful for stability research.

Conclusions

This study has compared local and marching solutions of the linear stability equations to determine how accurate local analysis is and how readily random disturbances collapse onto a unique asymptotic behavior. The differences between local and marching analyses are modest, fairly uniform in the cases studied, and permit local analysis to be used for engineering studies—possibly with an empirical correction. These differences may be attributed to the effect of history in causing the marched disturbance to lag behind the ideal which is a moving target that changes rapidly enough that it is not reached. To go farther will require knowing something about how disturbances are actually introduced and therefore what shape they are likely to have.

Some idea is given of the convergence of random disturbances to the asymptotic disturbance. The concern is raised that some disturbances can create arbitrarily large N factors and thus highlight the need for the solution to the receptivity problem.

Hall's conclusions that the first neutral point cannot be defined is supported by our results. The sensitivity of local solutions to ξ upstream of the local analysis neutral point is seen to prevent any rational definition of that point. It may not make sense to assign a unique growth rate anywhere in this part of the α, G plane. One must solve the receptivity problem here. Fortunately for N factor analysis, the exact location of a neutral curve is not as important as accurate growth rates farther downstream where rapid growth occurs.

Floryan[7] and Floryan and Saric[5] have compared the local analysis neutral curve and disturbance profile to experimental results by Bippes,[8] Wortmann,[9] Tani,[10] and Tani and Sakagami.[11] The neutral curve of the experiments by Bippes

lay outside that of the local analysis. The present work suggests the neutral curve at higher α should be shifted into the unstable region making it slightly smaller, thus, moving slightly in the wrong direction. Wortmann's neutral point is above Floryan's curve, but in a region where the present work is unable to justify any neutral curve. One is not surprised to find disagreement in a region so dependent on how disturbances get started.

There is also disagreement in v_m/u_m between Bippes and Floryan and Saric. The theoretical value is half the experimental. The marching result is smaller still, but by a factor of about 0.9 at the most. The differences between marching and local analyses are modest and are insufficient to explain the disagreement with experiments. However, the linear growth analysis is only one aspect of the overall stability analysis, and we need receptivitiy models to further the comparison with experiment.

For simplicity, no attempt has been made in this study to deal with other possible sources of discrepancies: the secondary effects of curvature, pressure gradients, non-Blasius boundary layers, and finite-amplitude disturbances.

Acknowledgments

The work was supported by the Office of Naval Research under Contract N00014-83-K-0098 and by the National Science Foundation under Contract MEA-8120935. The first author benefited greatly from discussions with J.M. Floryan, who also provided the program used to get the separation-of-variables solutions. Thanks are due to K. Herbert for programming support.

References

[1]Hall, P., "Taylor-Görtler Vortices in Fully Developed or Boundary-Layer Flows: Linear Theory," *Journal of Fluid Mechanics,* Vol. 124, 1982, pp. 475–495.

[2]Herbert, T., "On the Stability of the Boundary Layer Along a Concave Wall," *Archive of Mechanics,* Vol. 28, 1976, pp. 1039–1055.

[3]Hall, P., "The Linear Development of Görtler Vortices in Growing Boundary Layers," *Journal of Fluid Mechanics,* Vol. 130, 1983, pp. 41–58.

[4]Goldstein, S., *Modern Developments in Fluid Dyanamics,* Clarendon, Oxford, 1938, p. 119.

[5]Floryan, J. M., and Saric, W. S., "Stability of Görtler Vortices in Boundary Layers," *AIAA Journal,* Vol. 20, No. 3, 1982, pp. 316–324.

[6]Ragab, S. A., and Nayfeh, A. H., "Görtler Instability," *Physics of Fluids,* Vol. 24, 1981, pp. 1405–1417.

[7]Floryan, J. M., "Stability of Boundary-Layer Flows over Curved Walls," Ph Walls," Ph.D. Thesis, Virginia Polytechnic Institute and State Univ., Blacksburg, VA, 1980.

[8]Bippes, H., "Experimentelle Untersuchung des laminar-tubulenten Umschlags an einer parallel angeströmten konkaven Wand," Sitzungsberichte der Heidelberger Akademie der Wissenschaften, Mathematisch-naturwissenschaftliche Klasse, Vol. 3, 1972, pp. 103–180.

[9]Wortmann, F. X., "Experimental Investigations of Vortex Occurrence at Transition in Unstable Laminar Boundary Layers," Institut für Aerodynamik und Gasdynamik, Technische-Hoehschule Stuttgart, Stuttgart, Germany, Air Force Office of Scientific Research, Rept. 64-1280, AF 61 (052)-220, 1964.

[10]Tani, I., "Production of Longitudinal Vortices in the Boundary Layer along a Curved Wall," *Journal of Geophysical Research,* Vol. 67, 1962 pp. 3075–3080.

[11]Tani, I., and Sakagami, J., "Boundary-Layer Instability at Subsonic Speeds," *Proceedings of the International Council of Aeronautic Sciences, Third Congress,* Spartan, Washington, DC, 1964, pp. 391–403.